

**13-0417**

**Attempt to Further Enhance Ranging Accuracies to Lageos for the Next Generation Space Geodesy**

Thomas Varghese, Thomas Zagwodzki, Thomas Oldham, Sanhe Hu  
NASA Next Generation SLR Program /Cybioms Corporation  
Rockville, MD 20850, USA  
e-mail: [tvarghes@cybioms.com](mailto:tvarghes@cybioms.com)

**Abstract:**

*To improve the ranging accuracy to Lageos for the next generation satellite laser ranging (SLR) systems, a detailed analysis of the integrated response of the satellite was conducted for a state of the art ranging system. High bandwidth Lageos laboratory test data was used in conjunction with a satellite model to deduce the inferences. The target response to the ground station is the convolution of the spread function of the satellite with the laser transmitter and receiver detector temporal characteristics. From this, various detection scheme responses were computed and compared. Results are discussed.*

**Introduction**

The Global Geodetic Observing System (GGOS) requires high observing accuracies for SLR at the 1 mm level on geodetic satellites. The geodetic satellites operating today were launched during the last 3 decades. While satellites are expensive to manufacture and launch, those in orbit last for a long time and cannot be physically changed. Lageos 1 and 2, with its long history of geodetic ranging data and stable time series, have been the basis for the SLR contribution to ITRF. In this context, it is critical to examine the relevance, suitability, and adaptability of the current geodetic satellites for future high accuracy applications.

Lageos is designed to be point-mass objects in space with large mass to area ratio to enable Precision Orbit Determination (POD). To compute the precise orbits, precise ranges are needed to the Center of Mass of the satellite (CoM). Ideally, these satellites should behave as point optical targets in space. However, Lageos cannot behave as a point optical target in space due to its Laser Retro-reflector Array (LRA) structure. This structure has range accuracy dependencies on a variety of SLR system and satellite parameters. The “Fuzzy Range Depth Function” of the LRA and its strong dependencies on the SLR system configuration parameters require careful study to establish the framework for millimeter ranging accuracy. In this context of the emerging requirement for higher SLR accuracy, the Lageos 2 pre-launch NASA GSFC test data/ results [1] were examined to gain improved understanding on accuracies. The following sections describe the analysis efforts and some of the key findings.

**Analysis of the Laboratory Test Results and Simulations**

Prior to the launch, Lageos 1 and 2 were tested at the NASA Goddard Space Flight Center using the instrumentation available at that period. The extensive optical and the limited thermal measurements were done with a lot of care under the constraints of the laboratory setting. On-orbit conditions are extremely hard to simulate in the laboratory and hence limited simulations were done to examine the satellite behavior for on-orbit conditions.

Lageos, shown in Figure 1, is a spherical satellite (diameter of 600 mm) with a dense population of Total Internal Reflecting (TIR) corner cubes (426). The spherical satellite may be thought of as having polar (north and south) and equatorial regions. There is no LRA optical symmetry except about the poles of the satellite along the latitude. It is oriented along a preferred spin axis in its orbital plane and after decades of operation on orbit, the spin rate is now extremely small. A ground-based SLR station will see different regions of the satellite in a typical track. It will see a varying temporal response depending on whether the ground station line of sight is along the polar, equatorial, or in between regions.

For a plane wavefront illuminating the satellite, the Lidar returns from the cubes will coherently interact to generate a complex dynamic target impulse response [2] in the Far Field Diffraction Pattern (FFDP). Such a response will show significant variations in intensity, of an order of magnitude or more, depending on the polarization state of the illuminating beam and the thermal variations from the solar loading in space. The laboratory experiment could control the input laser polarization state, while the thermal conditions in space could be simulated only in a large vacuum chamber, which was not available.

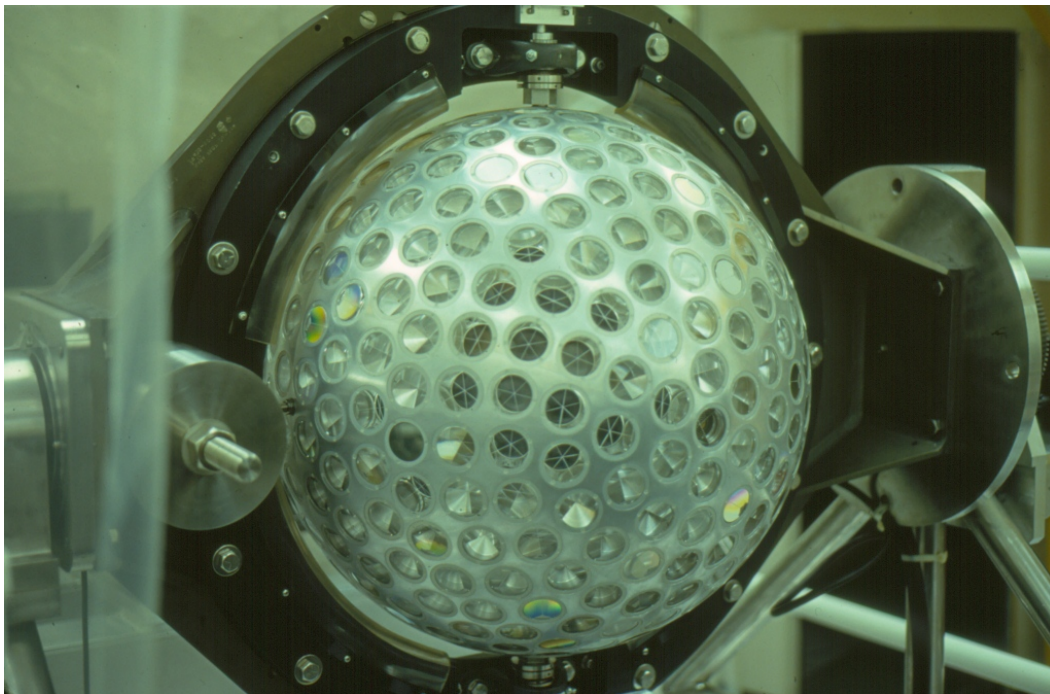
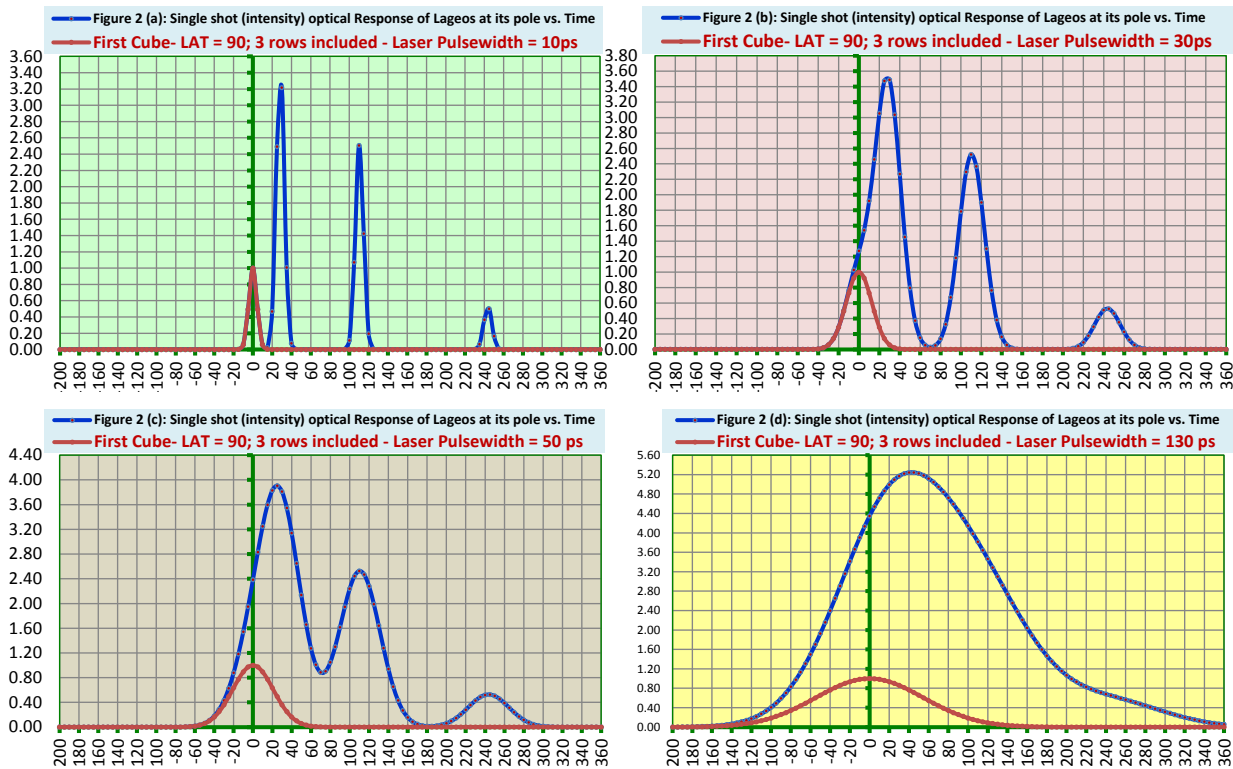


**Figure 1:** Lageos 2 mounted on a gimbal system at the NASA GSFC laboratory

To perform the original laboratory measurements, a timing reference pulse transferable to the surface of the satellite or the face of the cube normal to the incident beam via a calibration cube fixture was incorporated for the convenience of post-processing of the data. A collimated beam near diffraction limit illuminated the satellite in a highly confined optical path to minimize air currents. The return waveforms from the satellite were captured using a streak camera with a 2 picosecond temporal resolution (and better accuracy), with the input pulse always present on the sweep, thus serving as a reference. The streak camera digitized temporal waveform is an extremely accurate (low sub-millimeter) differential measurement of the reference pulse and

satellite response. This temporal waveform would have been fully resolved if very short ( $<10\text{ps}$ ) pulse lasers were used. In such a case, the resultant satellite response would be the impulse response of the satellite. However, due to the finite pulsewidth of the laser (30, 40, 60, 100 ps) used for testing, the obtained satellite response is wider from the convolution of the laser pulse temporal profile with that of the satellite impulse response.

As stated earlier, the input pulse was convenient at the beginning of the sweep as a temporal reference for aligning the pulses in the time domain prior to averaging the amplitudes to generate a single average waveform. Acceptable waveforms were then time synchronized digitally (via the reference pulse) for sample sizes  $> 200$ ). The timing computations were performed for peak-to-peak, half max-to-half max, and centroid-to-centroid of the averaged paired (reference and target) waveforms. The streak camera sweep nonlinearity correction (typically  $\pm 0.7$  picoseconds) is applied from a look up table for each of the above techniques. Also, a correction for latitude sag error was applied to all measurements as needed ( $\sim \pm 1.5\text{mm}$  @  $\pm 45$  deg).



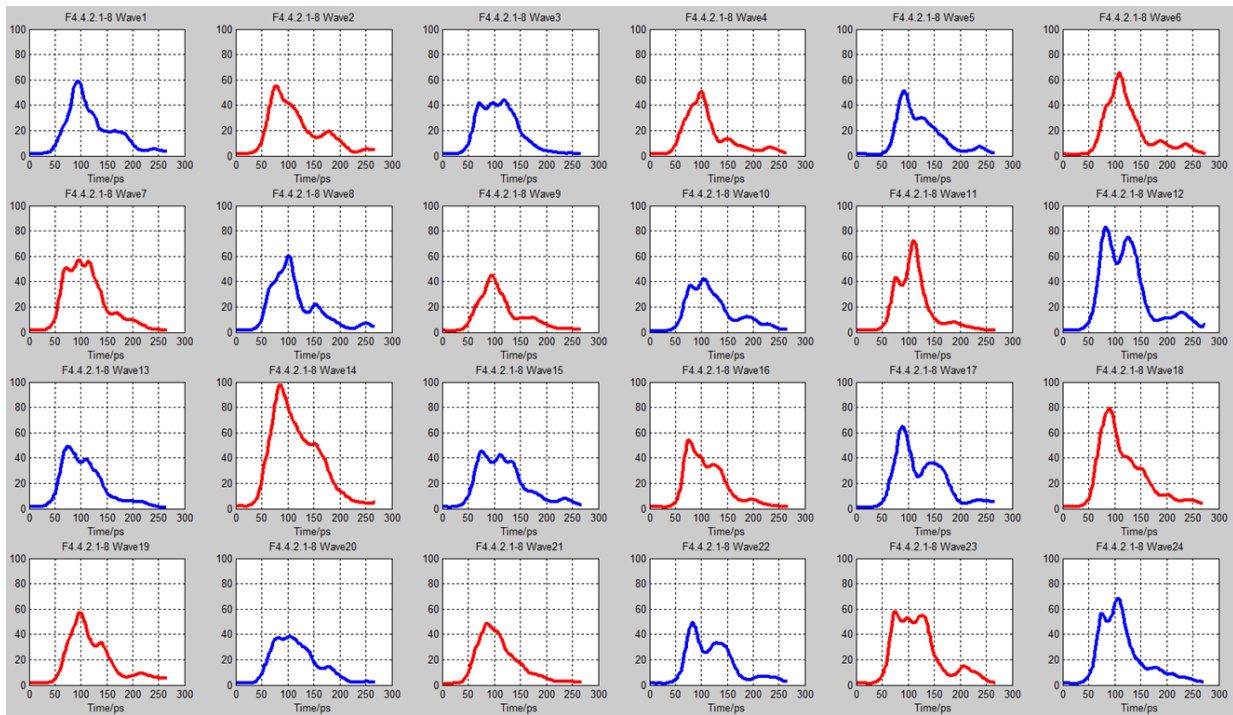
**Figure 2 (a) thru (d):** Simulation of the single shot response of the polar orientation of the satellite as a function of four pulse widths, viz., 10 ps, 30 ps, 50 ps, and 130 ps; horizontal scale is 10ps / division and the vertical scale is arbitrary for intensity.

Figure 2 illustrates the simulated single shot response of the satellite for the polar orientation of the satellite as a function of pulse width for 10, 30, 50, and 130 ps laser pulse widths for a single instance of the phasing of the cubes to illustrate the temporal structure of the satellite. The TIR cubes are oriented with random phasing within the satellite matrix. In this polar geometry, the nearest single cube provides the first pulse, while the next row of 6 produces the second pulse and so on. For the rows displaced farther and farther away from the pole cube, the effective lidar

cross-section decreases rapidly until total internal reflection is no longer possible. The best performance seen was up to the third row from the closest cube. The laser pulses also interact coherently to produce amplitude and temporal variations, which were evident from the temporal structure of the retro-reflected pulses from the satellite. The pulse shown in RED in Figure 2 is the reference input pulse and the pulses in BLUE indicate the corresponding target response of the satellite. Figure 2(a) has the RED and BLUE overlapping for the closest cube to the incoming beam. It can be seen that when the pulse width is very short, the pulses are fully resolved in the time domain, while a large input pulse width “absorbs” the satellite response into its pulse envelope. The amplitude and structure does vary from shot to shot in the FFDP region of interest due to the coherent interaction, resulting in the vector addition of amplitudes, producing variance in temporal structure.

### Center of Mass correction and SLR Accuracy

All simulations and most of the analysis discussed in this paper were performed using MATLAB. Fig. 3 shows the twenty four average waveforms computed from the measured satellite response for different satellite orientations by rotating the satellite in its gimbal system at a constant rate under computer control. The waveform, shown in each box, is the result of averaging over 200 waveforms taken during approximately 1 minute. In the real-world tracking of the satellite, the data will encompass different satellite orientations during a typical 10 minute segmented tracking with data averaging possible over the normal point bin.



**Figure 3:** Average waveform for different satellite orientations; the horizontal scale is 50 ps/ division and the vertical scale for intensity is arbitrary.

The rotation of the satellite in the fixture may be construed as equivalent to the motion of the satellite in its orbit. The actual tracking data obtained by the SLR station and the resulting normal

point (NPT) over a bin size of 120 seconds is thus equivalent to the computed average waveforms shown in Figure 3. The computed average waveform of the lab data offers an approximation of the on-orbit behavior of the satellite and its effect at the SLR normal point.

The “optical depth” in the satellite, to which ranging occurs, is heavily dependent on the input pulsewidth, signal detection level, and the detection scheme. A closer look at the high bandwidth waveforms from the lab data clearly shows that a small fraction of the leading edge is stable at all times and is least impacted by the variations introduced by the orientation differences. If the pulse is long, then the remaining part of the pulse profile succumbs to the amplitude and temporal variations within the satellite optical matrix and this is evident in the waveforms of the lab data. Thus, the range correction to the CoM has a strong dependency on the underlying SLR technologies and related engineering parameters. Detection schemes like the SPAD or MCP-PMT, signal processing algorithms like leading edge or centroid, and the detection signal regimes such as single photoelectron or multi-photoelectron do have a significant effect on the CoM correction mean value and its uncertainty.

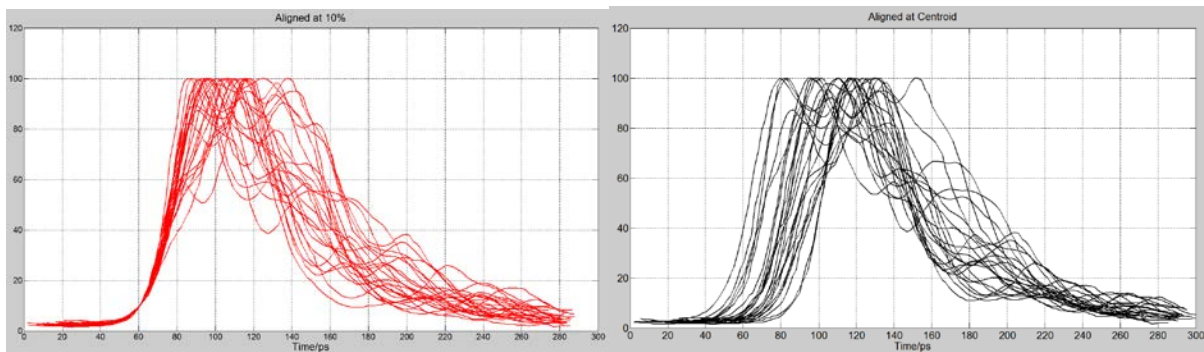


**Figure 4 (a) and (b):** Normalized waveforms after aligning the pulses for different detection schema; the horizontal scale is 20 ps/ division and the vertical scale is arbitrary for intensity. Figure 4(a) is the leading edge alignment at the 10% point, while 4(b) shows the alignment of the waveforms based on its centroid.

The laboratory experimental waveform taken under a non-saturating signal regime is an accurate representation of the response of the satellite for that instance and for the specific laser pulse attributes and satellite orientation. Even for a fixed orientation, the shot to shot variations were observed in the temporal profile of the satellite response due to variations of the temporal structure of the input laser pulse. As illustrated in Figure 3, there are significant differences in the average waveform among the various satellite orientations. Due to the optical depth function of the satellite, the satellite response is a highly skewed function for short (<50ps) input pulses. This has implications for the center of mass correction at the normal point level. If the detection rate is kept at a low percentage level, for example <5%, then the detection may be estimated to be at the single photoelectron level. The photon contributing to a single photoelectron may come randomly from anywhere within the satellite temporal response. This generation of the photoelectron from a random photon can be treated as a Markov process governed by Poisson statistics with a mean arrival rate. Even if the photoelectron arrival percentage is low on a shot to shot basis, if there is a substantial amount of data within the averaging normal point time bin, then the process of averaging of this large sample should produce a stable mean close to the

estimated value from the centroid algorithm. The opposite is true, if the sample size is small. In either case, however, the single shot RMS of the normal point will be higher compared to other detection schemes, as shown in Figure 4(b). This is particularly true for longer pulses with a pulsewidth  $> 10$ ps. Furthermore, for the centroid processing algorithm to work correctly, the iterative data editing cannot be tighter than a 3 sigma as truncation will cause shifting of the centroid and hence the CoM correction value. The leading edge approach focused on the waveform closest cubes is more deterministic (Figure 4a) and has a lower dispersion than other schemes such as centroid (Figure 4b) or peak detection.

When the input pulse is very short ( $<10$ ps), the satellite response is essentially the impulse response of the satellite. One can enable the triggering photon to occur on the leading edge of the first pulse by enabling a strong satellite link for a strong signal return. With the help of a very short ( $<10$ ps) laser pulse and a high precision ( $<1$ mm) ranging electronics, it is indeed possible to even collapse a multimodal residual data distribution into a single modal distribution by careful deconvolution / data translation based on satellite optical properties. This is evident from the Lageos test results as well as the MATLAB simulations performed. For a very short laser pulse, it is indeed possible to achieve a tighter NPT histogram by triggering on the leading edge as successfully demonstrated in Graz [3], where SLR is performed on Lageos with a  $\sim 10$  ps pulse and with no extra efforts to restrict the satellite return rate to a low percentage to confine to the weak signal regime. This indeed is the best approach as we can collect more SLR data without fear of any range error. On the other hand, centroid based single photoelectron detection scheme requires a low percentage of satellite return data combined with a minimum amount of data in the NPT bin for statistical robustness of the mean value. Sparse data in the NPT bin as well as non-uniform noise on the trailing edge of the NPT distribution could shift the mean range value and compromise the ranging accuracy to the CoM.

## Conclusion

The laboratory Lageos test data/results provide insights on ways to realize millimeter SLR accuracy from Lageos depending on the SLR station configuration parameters as well as embedded hardware technologies. The best accuracy is possible with the use of  $< 1$  millimeter (precision, accuracy) ranging electronics in combination with a very short ( $<10$  ps) circularly polarized laser. In general, for any short pulse widths, the leading edge of the retro-reflected pulse offers the most deterministic time reference for triggering ranging electronics, due to its farthest position away from the center of the satellite and immunity to array effects. With short pulses, one can resolve the satellite cubes in different rows, resulting in a multimodal range residual histogram, which can then be reprocessed to obtain a single distribution. An iterative, data editing ( $<3\sigma$ ) criteria may be applied to remove any asymmetric trailing edge of the range residual distribution to further tighten the normal point accuracy. Any skew in the data due to the detector may also be removed by deconvolution.

## References

1. *“Pre-launch Optical Characterization of Lageos 2”*, Minott, P.O., Zagwodzki, T.W., Varghese, T., Selden, M., NASA Technical paper 3400, Sep 1993.
2. *“Millimeter accuracy constraints on Lageos satellites and effective Ground Station solutions”*, Varghese, et.al. (to be published).
3. *Private Communication* (Georg Kirchner)